CHAPTER V
TEST RESULTS

5.1 Introduction

This chapter presents CERCHAR test results, scratching forces, and the groove volume observed on the specimen surfaces. These measurements contribute to a more comprehensive understanding of rock abrasivity and the relationship between bedding plane orientation, scratching direction, and the resulting wear characteristics.

5.2 CERCHAR abrasivity index

For each rock type CERCHAR test is performed on five specimens with different bedding plane orientations (α) and scratching directions (θ). Five scratching tests are performed under each bedding plane condition. The average wear width served as the input for determining the CERCHAR Abrasivity Index (CAI), as presented in Appendix B, which is computed using Equation (4.1) given in Chapter 4. The resulting CAI values are then categorized into abrasivity classifications according to the ASTM D7625-22 CERCHAR method, as presented in Table 5.1. Regarding of bedding plane orientation, stronger rocks (i.e. limestone) tend to show higher CAI values than the softer ones (i.e. gypsum).

The CAI results for all tested rock types, are plotted in Figure 5.1. They reveal clear effects of bedding plane orientations (α) and scratching directions (θ). In general CAI tends to increase with α angle. Argillaceous limestone and the two sandstones, however, show the highest CAI value at α = 0° and the lowest at α = 45°. This behavior does not show for bedded limestone and gypsum (Figure 5.1a). All rocks show similar effect of scratching directions with respect to bedding plane direction (Figure 5.1b). The lowest CAI value are obtained under θ = 0°. The abrasivity gradually increases to

the maximum at θ = 90°. Scratching parallel to bedding trends gives low abrasivity than that perpendicular to the beds.

Table 5.1 Average CAI and standard deviation.

Rock type	α (degrees)	θ (degrees)	CAI ± SD	Abrasiveness (ASTM D7625-22)
Khao Khad argillaceous limestone	0	-	2.54 ± 0.11	High
	45	90	1.86 ± 0.02	Medium
	90	0	1.61 ± 0.01	Medium
	90	45	1.76 ± 0.02	Medium
	90	90	1.99 ± 0.04	Medium
	135	90	2.20 ± 0.00	High
Khao Khad bedded limestone	0	-	1.17 ± 0.01	Medium
	45	90	1.20 ± 0.01	Medium
	90	0	1.07 ± 0.01	Medium
	90	45	1.10 ± 0.00	Medium
	90	90	1.26 ± 0.01	Medium
	135	90	1.28 ± 0.01	Medium
Phu Kadueng sandstone	0	-	1.90 ± 0.01	Medium
	45	90	1.39 ± 0.01	Medium
	90	0	1.16 ± 0.01	Medium
	90	45	1.32 ± 0.02	Medium
	90	90	1.55 ± 0.01	Medium
	135	90	1.63 ± 0.01	Medium
Phu Phan sandstone	0	-	1.63 ± 0.01	Medium
	45	90	1.13 ± 0.01	Medium
	90	0	0.93 ± 0.01	Low
	90	45	1.03 ± 0.01	Medium
	90	90	1.19 ± 0.01	Medium
	135	90	1.24 ± 0.01	Medium
Tak Fa gypsum	0	-	0.40 ± 0.00	Very low
	45	90	0.43 ± 0.01	Very low
	90	0	0.29 ± 0.01	Very low
	90	45	0.36 ± 0.02	Very low
	90	90	0.45 ± 0.00	Very low
	135	90	0.50 ± 0.03	Very low

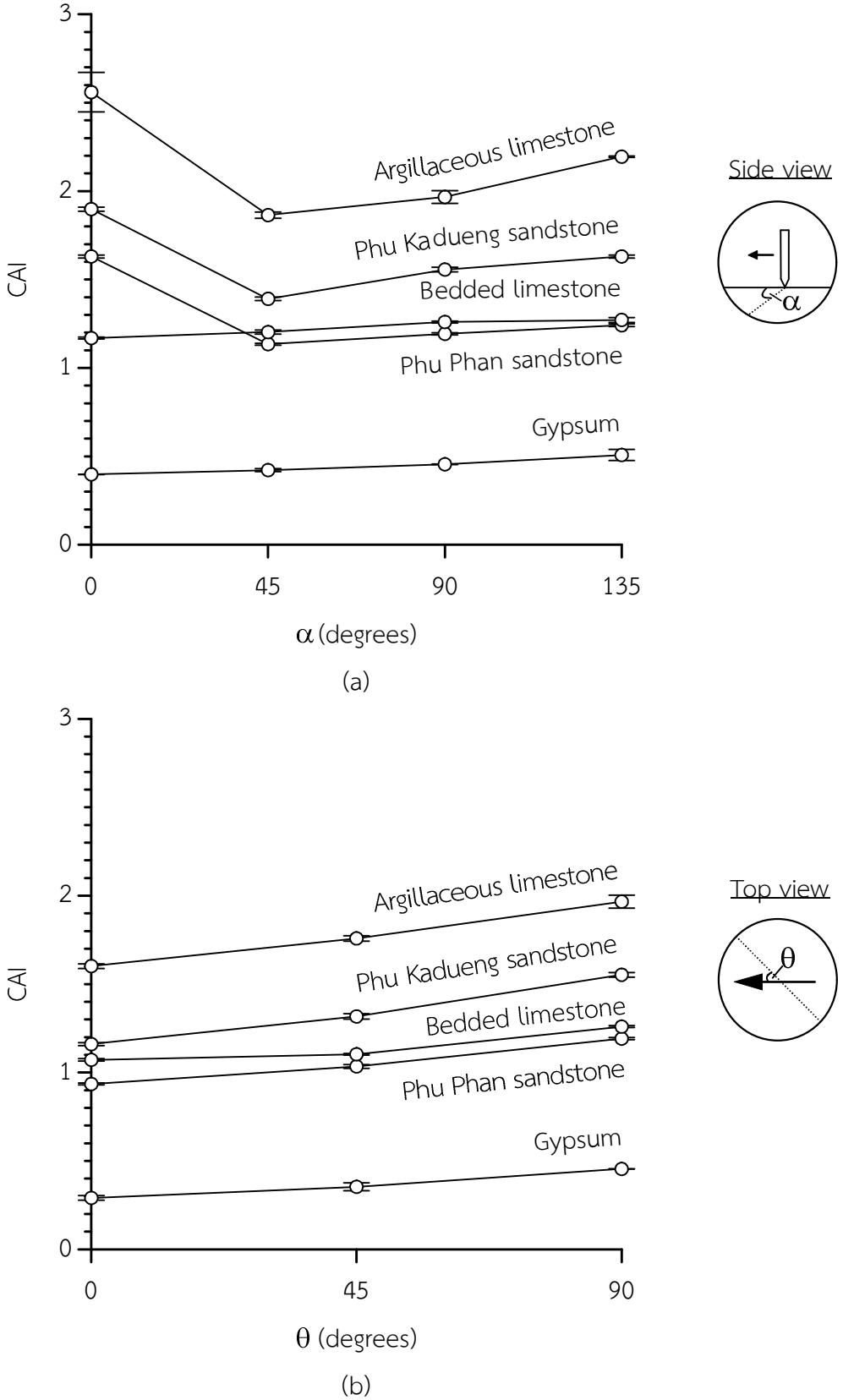

Figure 5.1 CAI as a function of bedding plane angle (a), and scratching direction (b).

5.3 Lateral force

Before obtaining the average lateral force, individual lateral force measurements for the five scratches have been recorded. These forces, derived from the rotational torque of the stylus pin, represent an additional parameter beyond those specified in the ASTM D7625-22 standard method. The lateral force values for each bedding plane condition are shown in Appendix C. The average lateral forces (F) as a function of scratching distance (d_s) for all test rocks are shown in Figures 5.2 through 5.6. For all rock types the scratching forces increase rapidly within the first 2-4 mm of scratching. Then they tend to remain constant with the distance. Stronger rocks (i.e. limestone and sandstone) show higher scratching force than the softer ones (i.e. gypsum). The effect of angle α on the scratching force is similar to those on the CAI value. The force generally increase with angle α. Scratching the stylus pin perpendicular to bedding plane trend (θ = 90°) show the largest force, as compared to those under θ = 0°. This holds trend for all rock types.

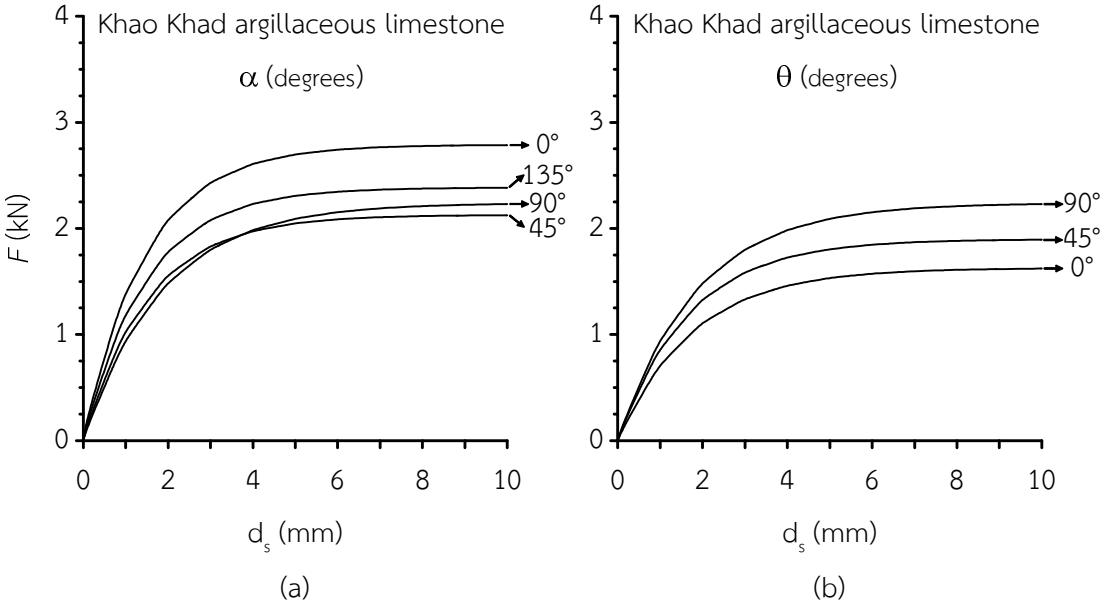

Figure 5.2 Scratching forces (F) as a function of scratching distance (d_s) of Khao Khad argillaceous limestone, bedding plane orientations (a) and scratching directions (b).

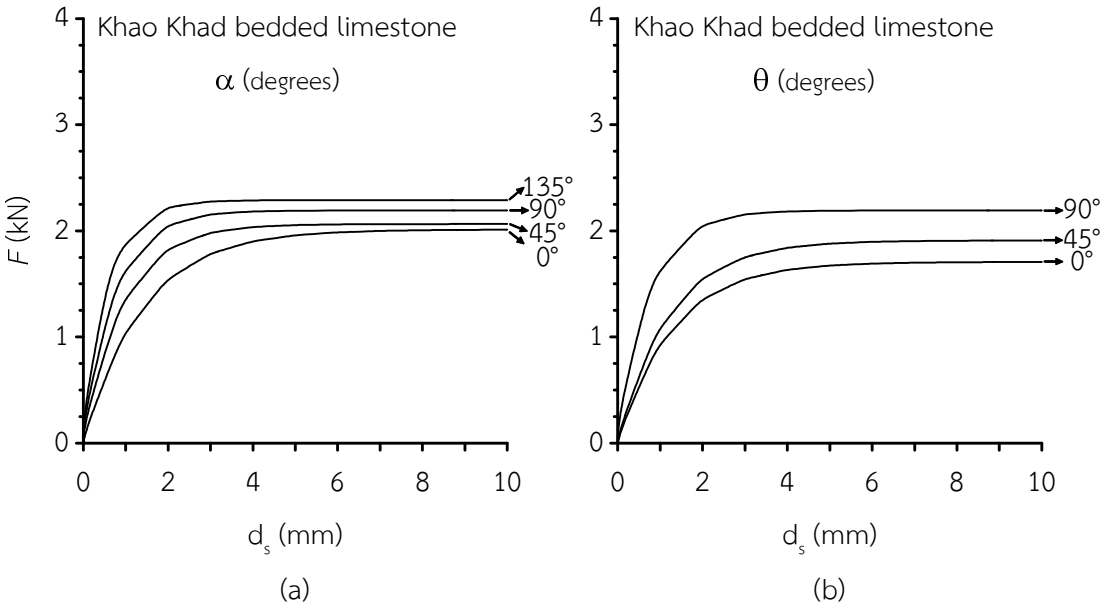

Figure 5.3 Scratching forces (F) as a function of scratching distance (d_s) of Khao Khad bedded limestone, bedding plane orientations (a) and scratching directions (b).

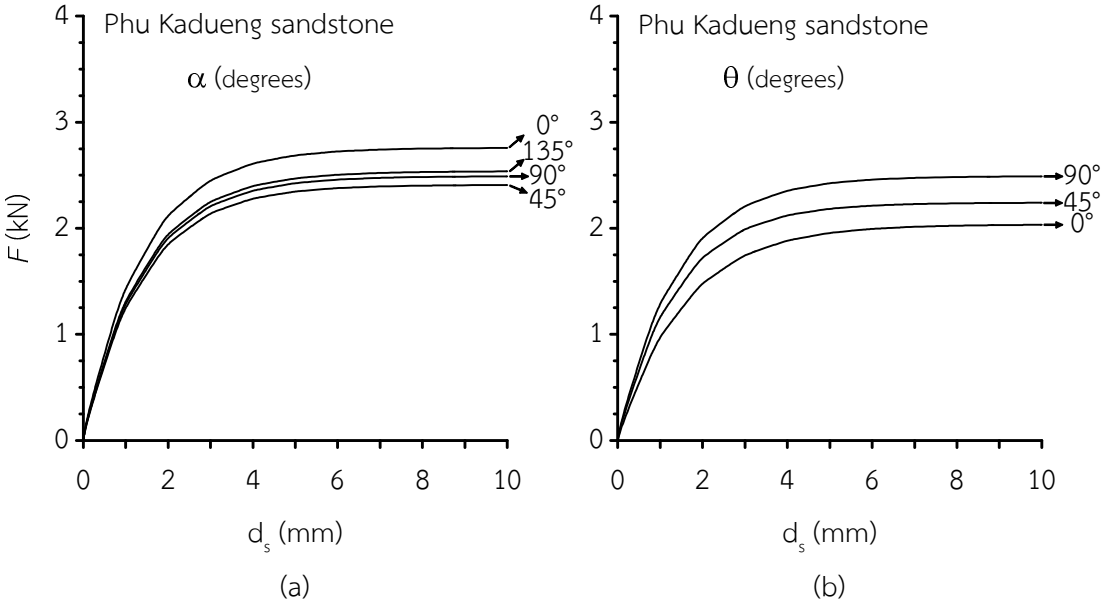

Figure 5.4 Scratching forces (F) as a function of scratching distance (d_s) of Phu Kadueng sandstone, bedding plane orientations (a) and scratching directions (b).

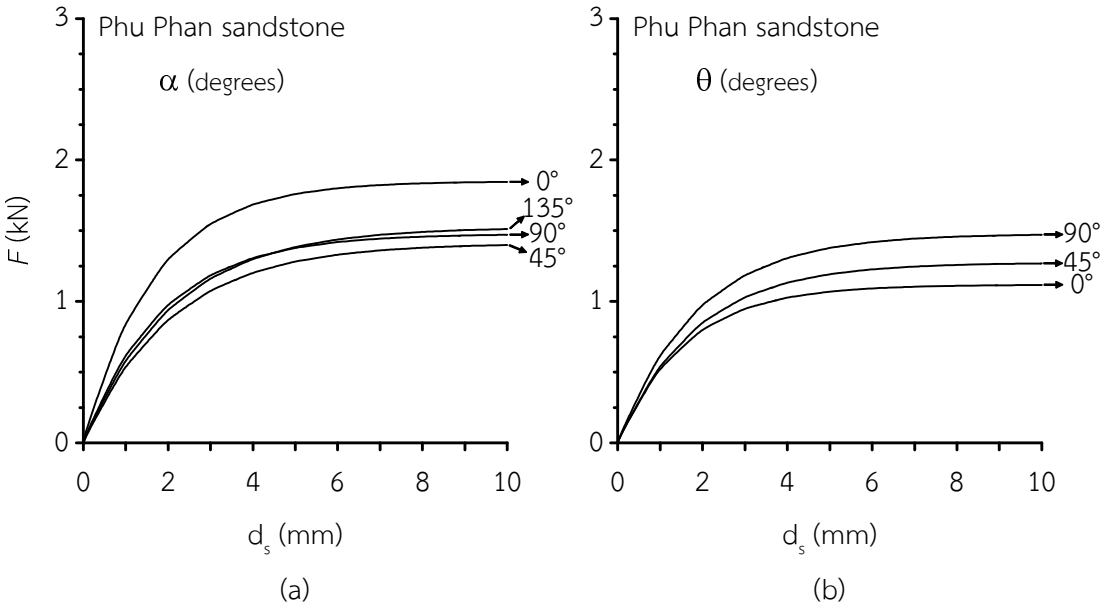

Figure 5.5 Scratching forces (F) as a function of scratching distance (d_s) of Phu Phan sandstone, bedding plane orientations (a) and scratching directions (b).

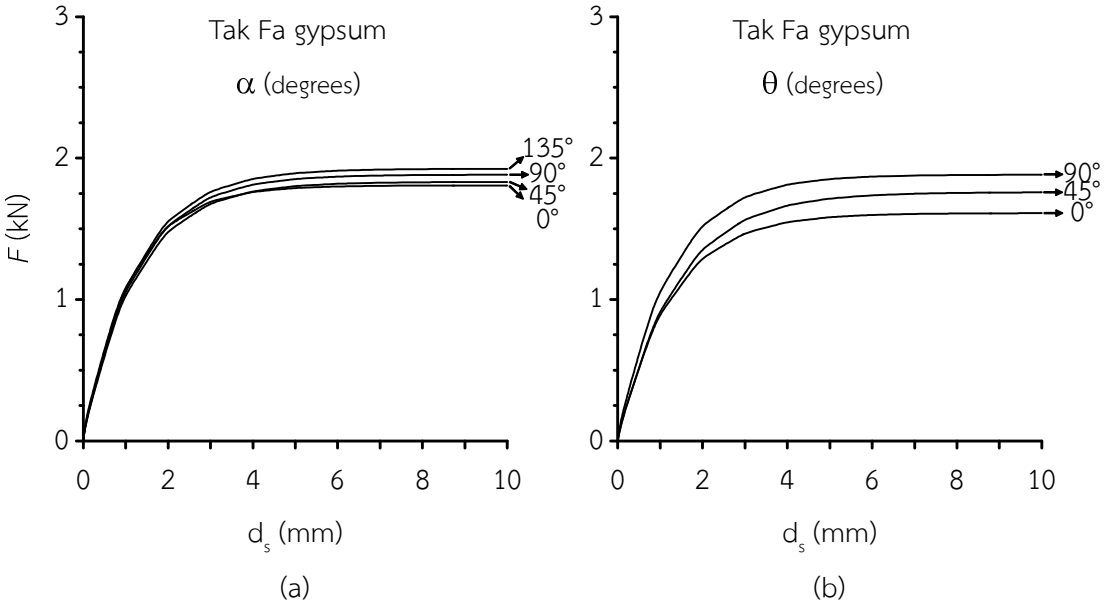

Figure 5.6 Scratching forces (F) as a function of scratching distance (d_s) of Tak Fa gypsum, bedding plane orientations (a) and scratching directions (b).

5.4 Groove volumes

The groove volumes for all tested rocks are averaged to obtain the mean groove volume (V) along with the corresponding standard deviation, Reflecting the results of rock's abrasivity characteristics. These results are summarized in Table 5.2, which provides a detailed comparison of the groove volumes across different rock types, highlighting variations with their bedding planes orientations and scratching directions.

As shown in Figure 5.7, higher groove volumes correspond to lower CAI values, as observed in Tak Fa gypsum (very low abrasiveness). However, a direct correlation between groove volume and CAI is not always evident, such as in the case of Phu Phan sandstone (medium abrasiveness), which shows groove volumes similar to those of Tak Fa gypsum. These discrepancies can be attributed to the mineralogical resistance to scratching, where bedding plane orientations and scratching directions align more consistently with the trends in CAI and lateral force for all test rocks. The groove images obtained from different bedding plane conditions are shown in Appendix C. Their corresponding values calculated form the method of laser scanning techniques explained in chapter IV are given in Figures D.1 – D.5 in Appendix D. Figure 5.7a shows the effect of bedding plane angle α on the groove volume. The maximum volumes are obtained with α = 45° for all rock types. Whereas softer rocks (i.e. gypsum and Phu Phan sandstone) show the largest scratching volumes, as compared to the stronger ones (such as limestone). Scratching the stylus pin parallel to bedding plane (θ = 0°) trend yields the largest volume. The lowest volumes are obtained when the stylus pin moves normal to the bedding plane trend (θ = 90°).

Table 5.2 Mean groove volumes for different angle α and θ.

Rock type	α (degrees)	θ (degrees)	Volume ± SD (mm^3)
Khao Khad argillaceous limestone	0	-	0.314 ± 0.03
	45	90	0.819 ± 0.06
	90	0	0.969 ± 0.04
	90	45	0.859 ± 0.05
	90	90	0.679 ± 0.05
	135	90	0.584 ± 0.04
Khao Khad bedded limestone	0	-	0.717 ± 0.02
	45	90	0.632 ± 0.04
	90	0	0.973 ± 0.06
	90	45	0.755 ± 0.03
	90	90	0.452 ± 0.02
	135	90	0.407 ± 0.07
Phu Kadueng Sandstone	0	-	0.536 ± 0.03
	45	90	0.846 ± 0.10
	90	0	1.097 ± 0.05
	90	45	0.900 ± 0.05
	90	90	0.768 ± 0.08
	135	90	0.635 ± 0.04
Phu Phan Sandstone	0	-	1.489 ± 0.10
	45	90	2.051 ± 0.04
	90	0	2.630 ± 0.12
	90	45	2.307 ± 0.05
	90	90	1.898 ± 0.03
	135	90	1.732 ± 0.08
Tak Fa Gypsum	0	-	1.899 ± 0.06
	45	90	1.931 ± 0.05
	90	0	2.501 ± 0.04
	90	45	2.243 ± 0.03
	90	90	1.889 ± 0.07
	135	90	1.706 ± 0.06

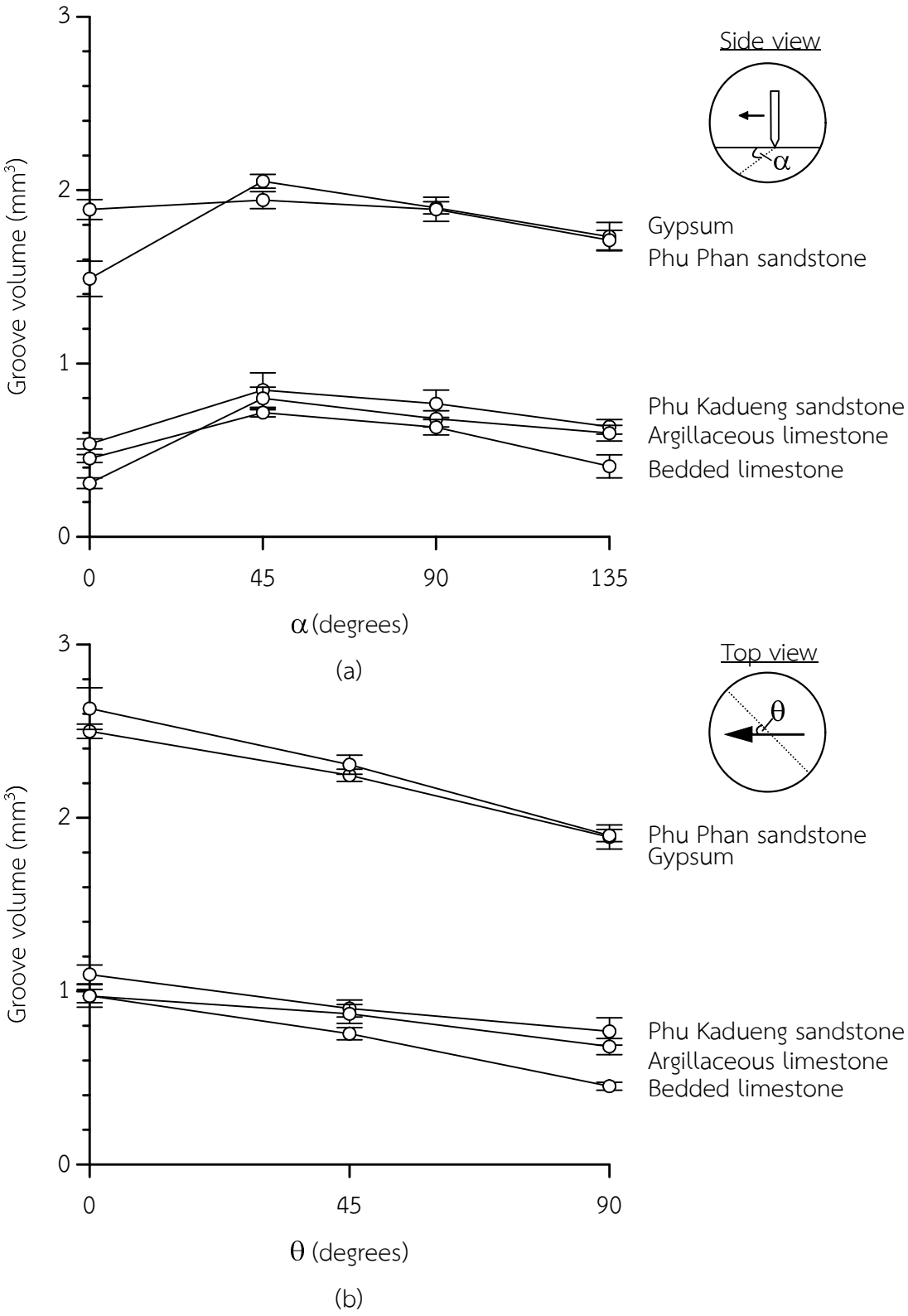

Figure 5.7 Mean groove volumes as a function of bedding plane orientations (a), and scratching directions (b).